Geological Society of America
Special Paper 349
2000

Lower-crustal cracking front at fast-spreading ridges: Evidence from the East Pacific Rise and the Oman ophiolite

Craig E. Manning
Department of Earth and Space Sciences, University of California, Los Angeles, California 90095-1567, USA
Christopher J. MacLeod
Department of Earth Sciences, Cardiff University, Cardiff CF1 3YE, UK
Patricia E. Weston
Department of Earth and Space Sciences, University of California, Los Angeles, California 90095-1567, USA

ABSTRACT

The earliest fracturing of lower-crustal gabbros in the Oman ophiolite and the East Pacific Rise occurred in a distributed, microscopic, semibrittle crack network that formed primarily at grain boundaries. The newly created permeability provided conduits that first delivered fluid to the lower crust and drove fluid + rock reactions. The abundance of metamorphic amphibole and modified magmatic plagioclase so produced ranges from trace quantities to >50 modal percent. The initial crack network differs in many respects from previous models. Amphibole and plagioclase compositions show that temperatures of initial cracking are high, ranging from ~700 °C near the dike-to-gabbro transition to ~825 °C near the petrologic Moho. An increase in temperatures of initial cracking with depth implies that strain rate increased with depth or that mineralogic controls on rheology or hydrolytic-weakening behavior varied through the crust. Comparison with thermal models shows that the semibrittle cracking front moves away from the ridge axis as it penetrates downward in the oceanic crust. For example, models involving rapid lower crustal cooling imply that the cracking front penetrates the dike-gabbro transition within ~1 km of the ridge and reaches the Moho within ~6 km. We suggest that microcracking occurred episodically because continuous advance of a cracking front over these distances implies velocities that are slow compared to reaction rates. The microscopic fracturing scale and inferred low fluid flux suggest that associated heat flow was conductive. These observations provide new insights into the brittle-plastic transition and fluid-rock interaction in the lower oceanic crust formed at fast-spreading ridges.

INTRODUCTION

The onset of fracturing is an important event in the evolution of the lower oceanic crust. In fast-spreading environments, where ductile shear zones are rare (Mével and Cannat, 1991; Gillis 1995; Manning and MacLeod, 1996), fracturing provides the initial permeability for the penetration of seawater into the lower crust. The onset of this mode of deformation also is associated with incipient seismicity. Models for the cooling of the oceanic lower crust suggest that fracturing begins at a downward-propagating "cracking front" that is associated with the initiation of brittle failure (Lister, 1974; Mével and Cannat, 1991). The earliest hydrothermal veins in ophiolitic gabbros have been interpreted as the fossil remnants of such a cracking front (e.g., Nehlig et al., 1988a, 1988b). However, these models have never been rigorously tested in ophiolitic or oceanic gabbros.

We have examined the earliest fracturing event in gabbros from two localities: Hess Deep, where East Pacific Rise lower crust has been exposed at the seafloor by normal faulting, and the Oman ophiolite, where lower-crustal sections are subaerially exposed. Lower crust at both localities was formed at high spreading rates so their comparison provides insights into the nature of the cracking front in mid-ocean ridge environments in which magma supply rates are high. Here, we show that the earliest brittle deformation in crust generated by fast spreading occurs at high temperatures during short-lived, distributed microfracturing events near the ridge axis.

GEOLOGIC BACKGROUND

Hess Deep

Hess Deep is a submarine rift valley in ca. 1 Ma crust that formed at the East Pacific Rise. Hess Deep lies at the western end of the Cocos-Nazca spreading center ~50–100 km east of the present East Pacific Rise spreading axis (Lonsdale, 1988; Francheteau et al., 1990). Exposed on the rift-valley walls and on fault blocks within the rift are ultramafic and gabbroic rocks, sheeted dikes, and pillow lavas, which formed at the East Pacific Rise at an inferred half spreading rate of 65 mm/yr (Francheteau et al., 1990). We examined Hess

Manning, C.E., MacLeod, C.J., and Weston, P.E., 2000, Lower-crustal cracking front at fast-spreading ridges: Evidence from the East Pacific Rise and the Oman ophiolite, *in* Dilek, Y., Moores, E.M., Elthon, D., and Nicolas, A., eds., Ophiolites and Oceanic Crust: New Insights from Field Studies and the Ocean Drilling Program: Boulder, Colorado, Geological Society of America Special Paper 349, p. 261–272.

Deep gabbroic rocks from two localities: Ocean Drilling Program (ODP) Hole 894G (2°18′N, 102°32′W), which was sited at an intrarift ridge; and samples collected during *Alvin* submersible dives on the northern scarp of the rift valley (2°21′N, 101°16′W; Karson et al., 1992; Gillis, 1995). ODP Hole 894G penetrated 154.5 m of gabbro, gabbronorite, and olivine gabbronorite (Gillis et al., 1993). The north-scarp samples include basaltic gabbro and gabbronorite. (All gabbroic rocks are referred to as gabbros for brevity.) Hole 894G gabbros are interpreted to have crystallized immediately beneath the typical stratigraphic position of the axial magma lens (Natland and Dick, 1996). The north-scarp rocks were collected a maximum of 300–700 m below the base of the sheeted dikes and are thought to have crystallized and cooled within or above the axial melt lens (Karson et al., 1992; Natland and Dick, 1996).

The Oman ophiolite

The middle Cretaceous Oman ophiolite has an internal structure that is similar to East Pacific Rise lithosphere exposed at Hess Deep. Numerous lines of evidence point to formation of Oman oceanic crust at a fast rate of spreading. U-Pb radiometric ages are similar throughout the ophiolite (Tilton et al., 1981). The crustal sequence is thick and continuous, and the restored orientation of the crust-mantle transition is perpendicular to that of the sheeted dikes. Plastic deformation, which is typical of amagmatic, axial disruption of the lower crust at slow-spreading ridges (Mével and Cannat, 1991), is rare in Oman gabbros (Pallister and Hopson, 1981; Lippard et al., 1986; Nicolas, 1989; MacLeod and Rothery, 1992). Finally, ubiquitous L-S crystal shape fabrics in the gabbros imply movement of crystal-liquid suspensions throughout the lower crust (Nicolas et al., 1988, 1994; Benn and Allard, 1989; Nicolas, 1989, 1992; Boudier et al., 1996), similar to magmatic flow fabrics in East Pacific Rise gabbros at Hess Deep (MacLeod et al., 1996).

For this study, we chose the Wadi Abyad section in the central part of the Oman ophiolite. This plutonic section was selected because it was affected less by spreading-ridge complexities (MacLeod and Rothery, 1992; Nicolas and Boudier, 1995) or obduction-related deformation than most areas in Oman. The sharp petrologic Moho and ~2.6-km-thick lower-crustal section are tilted ~30°N. The top of the plutonic sequence grades upward into the lowermost sheeted dikes, of which several hundred meters crop out. No higher levels are exposed in this area.

Detailed descriptions of the gabbroic rocks of Wadi Abyad are given by Browning (1982, 1984), Beurrier (1988), and MacLeod and Yaouancq (2000). Modally layered gabbros and olivine gabbros comprise the lower two-thirds of the plutonic section. Layering and layer-parallel foliation are parallel to the petrologic Moho. The layered gabbros pass up into foliated, massive, unlayered, medium-grained gabbro and olivine gabbro (~660 m thick). The dip of magmatic foliation increases within ~100–200 m of the base of the foliated gabbros, becoming nearly perpendicular to the Moho, and a steeply plunging lineation has developed. The foliated gabbros pass upward into 140 m of variably textured gabbro displaying extreme, meter-scale variability in texture and chemical composition. Subtle gradations among foliated, isotropic, and pegmatitic gabbro, microgabbro, and dolerite are observed. The upper boundary of the variably textured gabbros is gradational. It is marked by the absence of medium- to coarse-grained gabbros and by reduced grain size, such that microgabbros and dolerites predominate. The level corresponds to the dike-rooting zone described by previous authors elsewhere in the Oman ophiolite (Rothery, 1983; MacLeod and Rothery, 1992). This zone is the lowest level at which dikes have chilled margins.

Evolved, silica-rich plagiogranites and late wehrlites are volumetrically insignificant in the Wadi Abyad area. Rare north-northwest–trending to north-trending diabase dikes crosscut the section. Their depleted compositions suggest affinities to the younger "V2" lava series that postdates MORB-type "V1" lavas (Ernewein et al., 1988). The dikes are parallel to several dextral strike-slip faults and locally display mylonitic margins having dextral strike-slip offsets. Greenschist-facies alteration assemblages associated with dikes, faults, and parallel veins imply that this minor disruption of the section occurred at low temperatures, after the crust moved off the ridge axis. This later event may have been a manifestation of a slightly younger ridge segment or fossil propagating-ridge tip to the northwest (Juteau et al., 1988; Reuber et al., 1991; MacLeod and Rothery, 1992; Nicolas and Boudier, 1995).

MICROFRACTURING AND METAMORPHISM

In all samples studied from Hess Deep, the earliest gabbro metamorphism was associated with the development of a microfracture network (Manning and MacLeod, 1996; Manning et al., 1996). Gabbros from Wadi Abyad, Oman, display a similar, early microfracture network (Fig. 1). This event was the earliest in which secondary minerals formed because crosscutting relationships require that all other metamorphic events postdate the microfractures (e.g., Plate 2–1 in Manning and MacLeod, 1996).

The dominant microcrack morphologies are of the grain-boundary, intergrain, and intragrain type, in the terminology of Simmons and Richter (1976). Transgranular microcracks are rare. Intragrain microcracks are primarily evident as thin, planar arrays of healed fluid inclusions and micrometer-scale green to blue-green hornblende inclusions in plagioclase grains (Fig. 1, A and C). Grain-boundary microfractures are up to 40 μm wide, and porosity is entirely filled by green, blue-green, or brown hornblende (Fig. 1, A and B). On the scale of individual thin sections, the microcracks are evenly distributed throughout (Fig. 1, A and B). Shear offsets are rare (Fig. 1), pointing to an extensional, mode I origin for the crack network. Localization of deformation into fault zones or extensional fractures was not observed (later, crosscutting fractures do display such deformation localization as described subsequently). At larger scales of meters or more, the volumetric abundance of the microcracks, as expressed by changes in amphibole modal abundance, is quite variable in Hole 894G over ~150 m (Manning and MacLeod, 1996). However, a general decrease in the maximum volume of secondary-mineral formation occurs with increasing depth below the dike-gabbro transition in Wadi Abyad. This finding agrees with observations elsewhere in the Oman ophiolite (e.g., Gregory and Taylor, 1981; Stakes and Taylor, 1992).

Modification of primary magmatic minerals is spatially associated with microcracks. At the margins of microfractures, secondary calcic plagioclase rims occur on magmatic plagioclase (Fig. 1, C and D), and sporadic secondary calcic clinopyroxene replaces magmatic augite (Gillis, 1995; Manning and MacLeod, 1996). The extent of replacement of primary magmatic plagioclase is lower than that of mafic phases, resulting in larger amphibole patches where the latter are involved (Fig. 1). Figure 1D illustrates that on the microscopic scale, plagioclase recrystallization and grain-boundary modification are observed in Oman gabbros, similar to textures reported by Manning et al. (1996) for gabbros from Hess Deep. In samples from the north scarp of Hess Deep, chlorite locally postdates amphibole. It

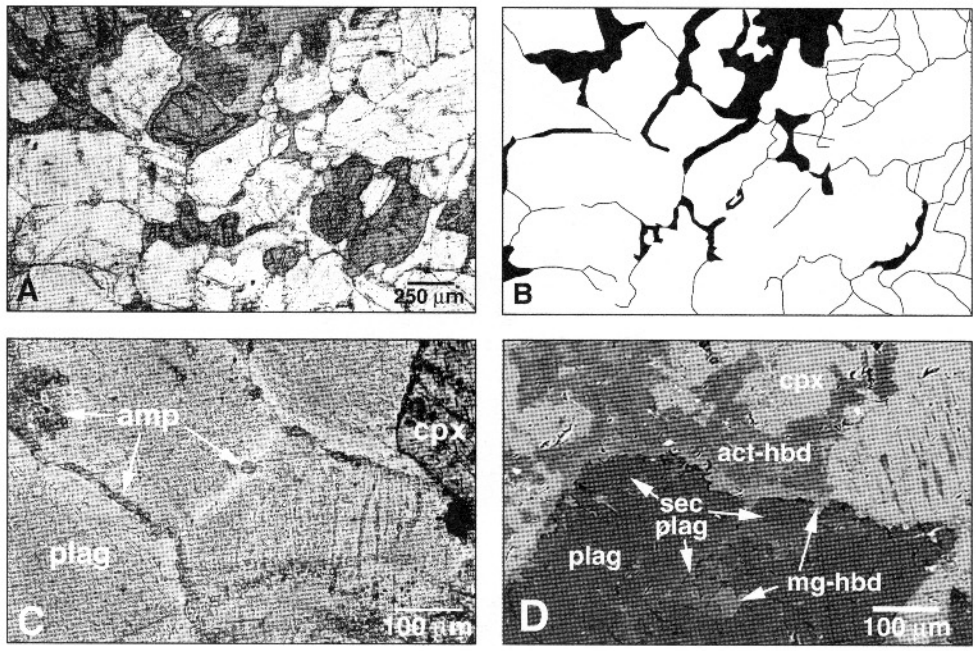

Figure 1. Textural characteristics of microscopic amphibole veins and associated alteration in gabbros from Wadi Abyad, Oman. A, Microscopic amphibole veins in foliated gabbro, sample Om75, plane-polarized light. Plagioclase grains are light, clinopyroxene, dark, and amphibole, intermediate. B, Line drawing of A at same scale showing amphibole-filled microcracks and alteration patches. Amphibole alteration is limited to narrow crack-filling zones along plagioclase-plagioclase grain boundaries, but is more extensive where clinopyroxene is involved owing to partial replacement of this phase. C, Healed fluid- and mineral-inclusion planes and grain-boundary microcracks, sample Om44, plane-polarized light. Abbreviations: amp—amphibole, cpx—clinopyroxene, plag—plagioclase. D, Backscattered-electron photomicrograph, sample Om75. Abbreviations: act-hbd—actinolitic hornblende, mg-hbd—magnesio-hornblende, cpx—clinopyroxene, plag—primary magmatic plagioclase, sec plag—secondary plagioclase. Higher intensity of backscattered electrons from magnesio-hornblende results from higher Fe content.

occurs both in grain-boundary regions and replacing plagioclase with little associated albitization. These areas were avoided in our analyses.

The coexistence of hornblende with calcic plagioclase and secondary clinopyroxene is diagnostic of the middle- to upper-amphibolite facies in mafic bulk compositions (Spear, 1981). The presence of chlorite with hornblende in the Hess Deep north-scarp samples (Gillis, 1995; Weston, 1998) suggests that metamorphism there continued to the greenschist-amphibolite transition.

Later fracture-related metamorphism occurred in both Hess Deep and in Wadi Abyad. In each locality, macroscopic fracturing followed microcracking. Macroscopic fractures are visible in outcrop and hand specimen as veins filled by secondary minerals. Macroscopic cracks are wider (millimeters to centimeters) than the microfractures. In addition, they are more continuous on the scale of decimeters to meters, and they cut across magmatic crystals rather than separating grain boundaries. In Hess Deep, progressively younger vein types are macroscopic amphibole veins, chlorite-bearing veins, and zeolite-calcite veins (Manning and MacLeod, 1996). In Wadi Abyad, later veins include macroscopic amphibole veins and epidote-bearing veins. In both localities, the later macroscopic fractures show that fracture deformation evolved from early distributed microcracking to later fracturing in which strain was localized into more widely spaced, throughgoing structures.

The evolution of fractures in Oman gabbros has been studied previously by Nehlig and Juteau (1988a, 1988b) and Nehlig (1994) in the Haylayn block to the northwest of Wadi Abyad. They described a macroscopic vein history similar to that which we observed in Wadi Abyad. However, they did not report alteration associated with microfractures. The intrusive history in the Haylayn area is more complex than that in Wadi Abyad. There is voluminous plagiogranite, and a large, late wehrlite intrusion cuts the section. The earliest fractures identified by Nehlig and Juteau (1988a, 1988b) are represented by voluminous actinolite veins. In light of the very high vein densities and the complex intrusive history in the Haylayn area, it is possible that early alteration related to microfractures has been overprinted and destroyed. In any event, because the macroscopic veins are younger than the earliest fracturing where we have observed crosscutting relationships (e.g., Manning and MacLeod, 1996), we assume that these veins were temporally distinct from the microcrack network that is the focus of this paper.

MINERAL COMPOSITIONS

Electron-microprobe analyses were performed on ten samples from Wadi Abyad and three samples from the north scarp of Hess Deep. Results were compared to those of Manning et al. (1996) on Hole 894G gabbros. The depth of the Oman samples ranged from the dike-gabbro transition to the Moho. Following Manning et al. (1996), amphibole and plagioclase compositions were determined at mutual grain edges such that analysis spots were <20 μm apart. Electron-microprobe operating conditions were 8 nA beam current, 15 kV accelerating potential, and 20 s counting times. A slightly defocused electron beam (~ 5 μm) was used for plagioclase analyses.

Standards were well-characterized natural and synthetic minerals. Oxide concentrations were derived by using a PAP correction algorithm (Pouchou and Pichoir, 1986).

Representative amphibole and plagioclase compositions are given in Tables 1 and 2, and key compositional parameters are plotted in Figure 2. The early amphiboles from Wadi Abyad and Hess Deep display a wide range in ^{IV}Al (Fig. 2). All amphiboles are calcic (Fig. 2C). In Hess Deep, X_{Mg} ranges from ~0.9 to ~0.6 in Hole 894G (Manning et al., 1996), but is lower (~0.7 to ~0.3) in the north-scarp samples because of higher bulk-rock Fe content (Fig. 2A). In Wadi Abyad, amphiboles are more magnesian (X_{Mg} = 0.7–0.9) at all levels except the dike-gabbro transition. As at the north scarp of Hess Deep, the gabbros at the highest levels are Fe rich, and this difference results in lower X_{Mg} values (0.6–0.7) of the secondary amphiboles. Amphibole in all samples displays an increase in A-site occupancy with ^{IV}Al (Fig. 2B). The substitution of ^{IV}Al for Si at low A-site occupancy (<0.2 atoms per formula unit) is tschermakitic, but at higher values is increasingly pargasitic.

The wide range of amphibole compositions illustrated in Figure 2, A–C, results from variations in bulk Al content on the grain scale (Manning and MacLeod, 1996). Where microcracks cut clinopyroxene, low bulk Al yielded actinolitic hornblende; where plagioclase was cut, more aluminous amphiboles grew. This difference can be seen in Figure 1D, in which magnesio-hornblendes (high-BSE [backscattered-electron] intensity) are in contact with plagioclase, and actinolitic hornblendes (low-BSE intensity) replace clinopyroxene. No compositional differences were discerned between amphiboles found within plagioclase crystals and those that occur at plagioclase-plagioclase grain contacts.

The compositional variability displayed by the amphiboles may seem inconsistent with growth at the high temperatures of the amphibolite facies. It is interesting that the compositional range reported here is not unique, but rather appears to be characteristic of amphibolite-facies amphiboles from oceanic gabbros (cf. Stakes and Vanko, 1986; Stakes et al., 1991; Stakes and Taylor, 1992; Gillis et al., 1993). This feature likely results from the combination of low strain and rapid reaction rates. Thus, the time scale for pore-filling reactions is faster than that required for transport-controlled development of homogeneous compositions of secondary minerals, consistent with formation at the high temperatures of the upper-amphibolite facies (discussed subsequently). It is important to note that growth of low-^{IV}Al actinolitic hornblende—and, locally, actinolite—at high temperatures is not inconsistent with this interpretation. Experimental studies show that Al-poor tremolitic amphibole is stable to >800 °C in Mg-rich, Al-poor bulk compositions (e.g., Jenkins, 1987), such as those represented on the microscopic scale by clinopyroxene and olivine grain-boundary environments in the gabbros.

Plagioclase compositions range widely in the sample suite (Fig. 2D). In samples from high levels of the gabbro section (i.e., both Hess Deep localities and the Oman samples from the dike-gabbro transition), average plagioclase compositions are $X_{An} \approx 0.55$. By contrast, samples from deeper in the gabbro section in Oman are significantly more calcic, with mean $X_{An} \approx 0.85$.

METAMORPHIC TEMPERATURES

Temperatures were calculated for compositionally appropriate amphibole-plagioclase pairs by using the extent of the $[NaSi]_{-1}[CaAl]$ exchange, as calibrated by Holland and Blundy (1994). Results are summarized in Table 3. Mean temperatures for amphibole-plagioclase equilibration in individual samples range from 711 to 829 °C. These temperatures are consistent with the inference from the mineral assemblage that metamorphism occurred in the upper-amphibolite facies (Spear, 1981).

Figure 3A shows temperatures as a function of stratigraphic position relative to the dike-gabbro transition. At Hess Deep, both sample suites are in high-level gabbros, near the dike-gabbro transition zone. Temperatures of initial fracturing in Hole 894G and the north scarp are statistically indistinguishable: 716 ± 5 °C and 711 ± 7 °C, respectively (uncertainties are standard errors in the mean). The samples from the same level in Wadi Abyad record nearly identical temperatures (Fig. 3A, Table 3). Samples from the foliated gabbros in Wadi Abyad yield somewhat higher temperatures of 754 ± 11 °C to 777 ± 10 °C. The two Oman samples from the deepest part of the lower crust near the Moho yield the highest temperatures (810 ± 5 °C and 829 ± 14 °C).

Two factors must be considered in assessing the accuracy of the inferred temperatures: equilibrium and thermometer applicability. First, it must be established that exchange equilibrium was closely approached at the time of fracturing and fluid flow, and that little subsequent exchange occurred. Manning et al. (1996) noted that metamorphism during fluid inflow after fracturing does not produce equilibrium textures because there is no penetrative deformation or grain-size modification. However, exchange equilibrium is likely to have occurred at the time of fracturing for three reasons: First, plagioclase shows textural evidence for re-equilibration during reaction with the fluid phase (Fig. 1D). Second, fluid + mineral reaction rates in the amphibolite facies result in equilibration on the time scale of days (Spear, 1981; Wood and Walther, 1983; Walther and Wood, 1984). Finally, $\delta^{18}O$ values of amphibole and plagioclase in Hess Deep and Oman gabbros are consistent with high-temperature equilibration with a fluid phase (e.g., Gregory and Taylor, 1981; Stakes and Taylor, 1992; Lécuyer and Gruau, 1996). Equilibration was local, on the scale of tens of micrometers, because amphibole compositions vary systematically as a function of grain-boundary mineral composition (Manning and MacLeod, 1996). Weston (1998) argued that diffusive re-equilibration during cooling is unlikely because of the sluggish diffusion rates in plagioclase and amphibole (e.g., Liu and Yund, 1992; Giletti and Casserly, 1994; Brabander and Giletti, 1995; Giletti and Shanahan, 1997).

The second factor influencing the accuracy of inferred temperatures is the compositional overlap between the data set used for geothermometer calibration and the gabbro data sets. All amphibole and plagioclase compositions in this study lie within the range of those used for calibration of the thermometer (see Manning et al., 1996). Compositional factors that might cause problems for the thermometer would be high concentrations of Mn, Ti, or halogens, as well as elevated cummingtonite substitution. Tables 1 and 2 show that the cation concentrations are low. Weston (1998) found that F and Cl contents are near detection limits in all studied samples. Likewise, cummingtonite substitution is low, as indicated by high Ca and Na in M4 sites (Tables 1 and 2).

In light of the apparent increase in temperature with depth exhibited in Wadi Abyad (Fig. 3), it is important to examine in more detail the plagioclase and amphibole compositions that suggest high temperature. Experimental investigations of the wet solidus of basalt by Helz (1973) equilibrated amphibole and plagioclase at 750–850 °C. Relevant compositional parameters of amphiboles are shown in Figure 2 for comparison with the Oman amphiboles. At oxygen fugacities of Ni-NiO, similar ^{IV}Al, ^{M4}Na, and A-site occupancy were observed. Minor differences in X_{Mg} are probably attributable to bulk compositional differences (the layered gabbros in Oman are cumu-

TABLE 1. REPRESENTATIVE AMPHIBOLE AND PLAGIOCLASE ANALYSES FROM HESS DEEP

	ODP Hole 894G–Interrift Ridge										*Alvin* dive samples–North Scarp					
Sample	4R-02-7		8R-01-10		9R-04-11		13R-01–11B		17R-02-1B		2213-1125		2218-1323		2213-1053	
analysis	50	51	16A2	17P2	20	21	48A1	49P1	8A	8P	68	69	52	51	8	9
phase	amp	plag	amp	plag	amp	plag	amp	plag	amp	plag	amp	plag	amp	plag	amp	plag
SiO_2	43.92	56.26	47.73	55.67	43.98	49.98	47.11	53.90	50.65	50.68	49.71	52.48	45.46	58.36	52.66	55.94
TiO_2	00.56	00.04	00.82	00.05	00.27	00.02	00.29	00.00	00.33	00.04	0.40	0.05	1.17	0.00	0.33	0.05
Al_2O_3	10.46	26.92	06.74	27.30	12.66	30.95	09.10	28.10	05.08	31.40	4.64	30.03	6.63	26.18	3.82	27.24
Cr_2O_3	00.02	0.00	00.04	00.02	00.01	00.00	00.08	00.02	00.00	00.05	0.08	0.05	0.00	0.00	0.00	0.00
FeO	17.69	00.33	15.91	00.56	11.79	00.67	13.41	00.58	12.32	00.39	17.54	0.39	21.66	0.31	13.85	0.69
MnO	00.19	00.07	00.24	00.07	00.27	00.05	00.26	00.01	00.18	00.01	0.52	0.03	0.41	0.02	0.24	0.00
MgO	10.20	00.01	12.11	00.00	14.43	00.15	13.62	00.00	15.02	00.00	12.68	0.00	8.50	0.00	14.75	0.06
CaO	11.80	09.74	11.44	09.97	10.95	14.48	11.32	10.95	11.94	14.40	10.59	12.77	11.20	7.64	11.47	10.59
Na_2O	01.97	05.85	01.31	06.01	02.56	03.30	01.34	05.19	00.84	03.62	0.65	4.12	1.06	7.23	0.50	5.21
K_2O	00.20	00.46	00.18	00.04	00.12	00.00	00.16	00.03	00.11	00.01	0.03	0.04	0.17	0.06	0.07	0.05
Total	97.01	99.69	96.52	99.69	97.04	99.60	96.69	98.78	96.47	100.60	96.83	99.94	96.26	99.80	97.67	99.82
Si	6.574	2.546	7.072	2.523	6.348	2.298	6.851	2.470	7.350	2.302	7.349	2.384	6.943	2.617	7.587	2.529
IV_{Al}	1.426	1.436	0.928	1.458	1.652	1.678	1.149	1.518	0.650	1.681	0.651	1.608	1.057	1.384	0.413	1.452
VI_{Al}	0.420		0.249		0.502		0.411		0.219		0.158		0.137		0.236	
Ti	0.063	0.001	0.091	0.002	0.029	0.001	0.032	0.000	0.036	0.001	0.044	0.002	0.134	0.000	0.036	0.002
Cr	0.002	0.000	0.005	0.001	0.001	0.000	0.009	0.001	0.000	0.002	0.009	0.002	0.000	0.000	0.000	0.000
Fe^{3+}	0.485	0.006	0.407	0.011	0.782	0.013	0.597	0.011	0.345	0.007	0.369	0.007	0.590	0.006	0.141	0.013
Fe^{2+}	1.730		1.564		0.642		1.034		1.150		1.799		2.176		1.528	
Mn	0.024	0.003	0.030	0.003	0.033	0.002	0.032	0.000	0.022	0.000	0.065	0.001	0.053	0.001	0.029	0.000
Mg	2.275	0.001	2.674	0.000	3.104	0.010	2.952	0.000	3.248	0.000	2.794	0.000	1.935	0.000	3.167	0.004
Ca	1.893	0.472	1.816	0.484	1.693	0.713	1.764	0.538	1.857	0.701	1.678	0.622	1.833	0.367	1.771	0.513
Na	0.572	0.513	0.376	0.528	0.716	0.294	0.378	0.461	0.236	0.319	0.186	0.363	0.314	0.629	0.140	0.457
K	0.038	0.027	0.034	0.002	0.022	0.000	0.030	0.002	0.020	0.001	0.006	0.002	0.033	0.003	0.013	0.003
Total	15.502	5.005	15.246	5.011	15.524	5.009	15.239	5.001	15.133	5.014	15.108	4.992	15.205	5.007	15.061	4.973
T (°C)	724		737		818		718		727		721		733		673	

Note: Amphibole formulae were normalized to 23 anhydrous oxygens, and then Fe^{3+} contents were calculated by following Holland and Blundy (1994); values given are the midpoints between maximum and minimum required by charge balance (Holland and Blundy, 1994). All Fe assumed to be Fe^{3-} in plagioclase. Oxide concentrations listed as 0.00 wt% are below detection.

TABLE 2. REPRESENTATIVE AMPHIBOLE AND PLAGIOCLASE ANALYSES FROM OMAN OPHIOLITE

	Wadi Abyad											
Sample	Om1		Om7		Om41		Om68		Om72		Om86a	
analysis	12	10	59		27	26	84	85	104	105	33	34
phase	amp	plag	amp	58	amp	plag	amp	plag	amp	plag	amp	plag
SiO_2	55.54	48.57	44.75	49.29	46.76	46.64	52.44	47.95	55.03	48.70	44.93	53.51
TiO_2	0.33	0.02	0.10	0.00	0.32	0.00	0.30	0.03	0.36	0.03	0.34	0.08
Al_2O_3	2.65	31.35	12.54	32.42	10.09	34.37	5.23	33.17	2.71	33.24	10.06	28.47
Cr_2O_3	0.37	0.00	0.09	0.00	0.01	0.00	0.16	0.03	0.11	0.00	0.01	0.07
FeO	4.95	0.18	11.35	0.30	12.32	0.13	8.47	0.37	6.08	0.32	17.29	0.66
MnO	0.11	0.01	0.20	0.00	0.17	0.02	0.06	0.04	0.11	0.00	0.21	0.06
MgO	20.67	0.06	13.99	0.00	14.25	0.00	17.97	0.00	20.23	0.00	10.85	0.00
CaO	12.43	16.80	11.96	15.73	12.42	18.13	12.31	16.88	12.45	16.44	11.27	11.44
Na_2O	0.66	2.41	2.46	2.74	2.08	1.61	1.01	2.22	0.49	2.50	1.53	5.17
K_2O	0.01	0.00	0.07	0.00	0.04	0.00	0.01	0.00	0.04	0.00	0.13	0.12
Total	97.72	99.41	97.51	100.48	98.46	100.89	97.97	100.70	97.61	101.23	96.62	99.57
Si	7.692	2.244	6.459	2.246	6.705	2.131	7.350	2.191	7.660	2.209	6.671	2.443
IV_{Al}	0.308	1.708	1.541	1.742	1.295	1.851	0.650	1.787	0.340	1.777	1.329	1.532
VI_{Al}	0.125		0.592		0.411		0.214		0.105		0.432	
Ti	0.034	0.001	0.011	0.000	0.035	0.000	0.032	0.001	0.038	0.001	0.038	0.003
Cr	0.041	0.000	0.010	0.000	0.001	0.000	0.018	0.001	0.012	0.000	0.001	0.003
Fe^{3+}	0.102	0.004	0.482	0.006	0.430	0.002	0.348	0.007	0.150	0.006	0.680	0.013
Fe^{2+}	0.471		0.888		1.047		0.645		0.558		1.467	
Mn	0.013	0.001	0.024	0.000	0.021	0.001	0.007	0.001	0.013	0.000	0.026	0.002
Mg	4.266	0.004	3.009	0.000	3.045	0.000	3.754	0.000	4.197	0.000	2.401	0.000
Ca	1.845	0.832	1.850	0.768	1.908	0.887	1.849	0.826	1.857	0.799	1.793	0.559
Na	0.177	0.216	0.688	0.242	0.578	0.142	0.274	0.197	0.132	0.220	0.440	0.457
K	0.002	0.000	0.013	0.000	0.007	0.000	0.002	0.000	0.007	0.000	0.025	0.007
Total	15.076	5.009	15.567	5.004	15.483	5.015	15.143	5.012	15.069	5.012	15.303	5.019
T (°C)	780		752		788		773		760		734	

Note: See Table 1 for analytical notes.

lates and, therefore, not of basaltic bulk composition). Mole fractions of anorthite are also comparable in the experimental charges and the Oman gabbros. Thus, the high temperatures inferred for the base of the gabbro section in Wadi Abyad are interpreted as an accurate assessment of the onset of fracture-related metamorphism.

DISCUSSION

Origin of microcracks by semibrittle failure

A distributed microfracture network is found in all Hess Deep and Oman gabbros studied. Failure by distributed microcracking therefore appears to be a volumetrically significant deformation mechanism for the lower crust at fast spreading rates. Macroscopic failure modes may be of three types (e.g., Rutter, 1986; Evans et al., 1990): brittle, semibrittle, and plastic. Petrographic characteristics of brittle failure include localization of strain into throughgoing fracture surfaces, microcracking, and textural indications of frictional sliding. Evidence for deformation by plastic flow includes crystal-plastic features such as twinning and undulatory extinction, and deformation is macroscopically homogeneous. Semibrittle flow involves deformation by a combination of microfracturing and crystal plasticity, leading to a macroscopically homogeneous distribution of deformation. On the basis of the dilatant, microscopic, distributed nature of the microfracture networks in Oman and Hess Deep gabbros, we infer that they represent deformation in the semibrittle field. Although we have not carried out a systematic study of the crystal-plastic textures that should accompany the microcracks, we note that patchy, undulose extinction and minor deformation lamellae in plagioclase and augite occur in the Oman gabbros (Wilks and Carter, 1986). As the formation of metamorphic amphibole in the gabbros was associated with the microcracks, it is evident that hydrothermal hydration of the lower crust occurred during semibrittle deformation, after the gabbros had cooled below the brittle-plastic transition.

Microcracking temperatures and their variation with depth

Given that metamorphism was associated with microcracking, metamorphic temperatures can be used to study the pattern of development of semibrittle deformation in the oceanic lower crust. Detailed statistical analyses have been carried out for the metamorphic temperatures associated with microfracturing in both Hess Deep localities (Hole 894G, Manning et al., 1996; north scarp, Weston, 1998). These studies reveal that metamorphism related to microfracturing in each locality very likely occurred in a single event. This is because F-tests show the small standard deviations of each temperature population to be consistent with a single underlying distribution at the 90% confidence level. Moreover, χ^2 and Kolmogorov-Smirnov tests indicate that the north-scarp and Hole 894G populations are not statistically distinct (Weston, 1998). This result implies that despite their geographic separation, the early metamorphic event occurred over the same temperature interval, which was no more than 66 °C (748–682 °C) at the 90% confidence level.

Statistical analyses of similar detail have not been carried out for the Oman sample suite. However, examination of the standard deviations permits preliminary conclusions about early metamorphism in Wadi Abyad. Table 3 shows that the standard deviations of the temperature populations in each sample are, with one exception (Om65), similar to or less than that of the thermometer-calibration data set (39 °C). This result implies that, like Hess Deep, the Oman samples record a single, narrow temperature distribution.

Figure 3A shows that metamorphism of the Oman gabbros was

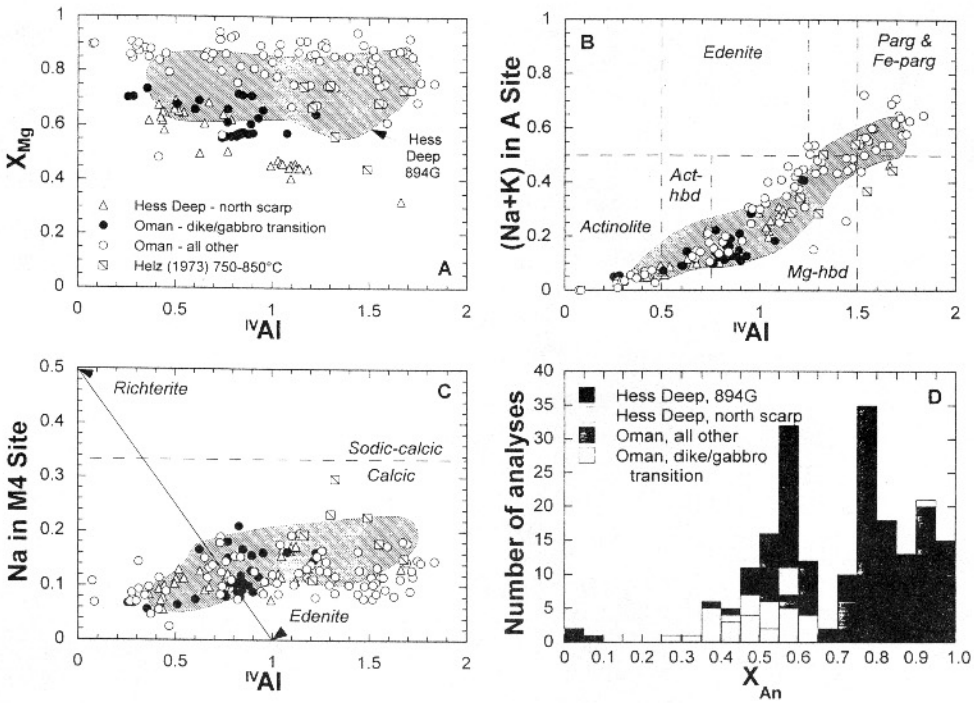

Figure 2. Amphibole and plagioclase compositional parameters. Amphibole nomenclature after Leake (1978). A, Mole fraction of Mg [X_{Mg} = Mg/(Mg + Fe^{2+})] vs. tetrahedrally coordinated Al (^{IV}Al) in amphiboles. B, Alkali cations in A site vs. ^{IV}Al in amphiboles; symbols as in A. Act-hbd—actinolitic hornblende, Mg-hbd—magnesio-hornblende, Parg—pargasitic hornblende, Fe-parg—ferropargasitic hornblende. C, Na in M4 site vs. ^{IV}Al in amphiboles with richterite-edenite exchange trajectory used in temperature determination. Near-linear increase in ^{M4}Na indicates that extent of richterite-edenite exchange is similar for all amphiboles, consistent with narrow calculated temperature interval. Symbols as in A. D, Histogram of plagioclase compositions in terms of mole fraction of anorthite [X_{An} = Ca/(Ca + Na)].

TABLE 3. TEMPERATURES OF INITIAL CRACKING

Location and sample	Depth below dike-gabbro transition (km)	Number of analyses	Mean T (°C)	Standard deviation	Standard error in mean	Notes
Hess Deep						
Hole 894G	0–1	52	716	36	5	Manning et al. (1996)
North Scarp	0–0.3	29	711	37	7	
Oman						
Om86	0.15	11	708	31	9	
Om75	0.42	9	715	36	12	
Om72	0.59	9	777	31	10	
Om68	0.67	8	754	29	11	
Om65	0.83	6	756	59	24	
Om07	1.05	9	769	31	10	
Om53	1.08	8	—	—	—	$X_{an} > 0.9$
Om48	2.22	3	—	—	—	$X_{an} > 0.9$
Om41	2.34	4	810	9	5	
Om01	2.60	8	829	38	14	

Note: Temperatures not calculated for samples in which $X_{an} > 0.9$ because this composition is outside the calibration range of the thermometer (Holland and Blundy, 1994). Pressure was assumed to be 1 kbar.

comparable to that at Hess Deep, in that similar temperatures are recorded at the same levels. In addition, the deeper levels exposed in Wadi Abyad imply that the metamorphic event caused by microfracturing occurred at progressively higher temperatures with increasing depth in the crust. Taking temperature to be the independent variable, a second-order polynomial yields an equation for the variation in depth below the dike-gabbro transition (z, in km) with temperature (T, in °C): $z = 76 - 0.22T + (1.5 \times 10^{-4})T^2$, and $R^2 = 0.93$ (Fig. 3B). (Hole 894G data were omitted from this fit because of their large depth uncertainty; however, they are consistent with it.) A linear fit gives lower R^2 (0.85) and systematic deviations at low and high z; a higher-order polynomial is probably unwarranted for the size of the data set and the precision of individual determinations. The polynomial is strictly applicable only to Wadi Abyad, because crustal thickness may vary from locality to locality. Nevertheless, if Hess Deep and Wadi Abyad gabbros are representative, the fit implies that there is a nonlinear increase in temperature of the onset of semibrittle deformation in the lower crust of fast-spreading ridges.

Constraints on the cracking front in the lower crust

The Lister model. Lister (1974, 1982) developed a conceptual model for the penetration of water into cooling crust near oceanic ridges. In this model, fluid influx occurs via permeability generated by a cracking front that propagates downward into fresh, uncracked rock. Fracturing occurs when tensile stress due to cooling and contraction slightly exceeds overburden stress. Lister envisioned that the cracking front could affect the entire crustal section and the upper mantle, though he recognized that it would penetrate below the dike-gabbro transition only after the lithospheric section had moved off

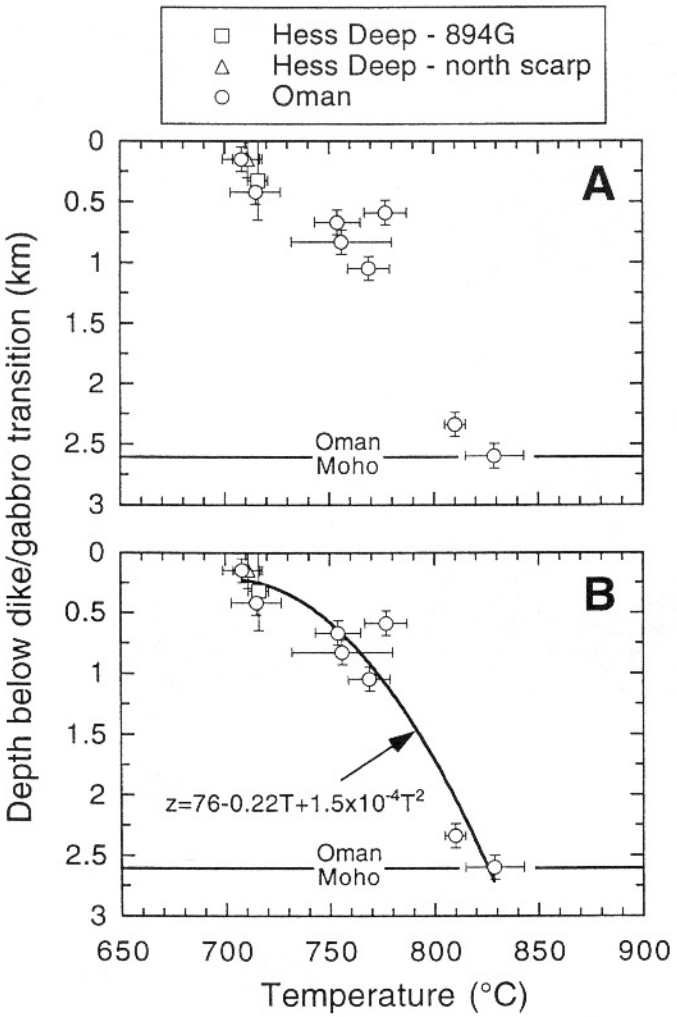

Figure 3. A, Variation in mean temperature of amphibole-plagioclase equilibration in microcracks with depth below dike-gabbro transition in Hess Deep and Oman. Temperature uncertainties are standard error of the mean (Table 3). Hole 894G mean is plotted at midpoint of an assumed possible depth range of 0–0.75 km below dike-gabbro transition. B, Same as A, with least-squares fit.

axis. Mével and Cannat (1991) elaborated on this model by pointing out that spreading rate should play a role in determining how water enters the lower crust. At slow-spreading ridges, high-temperature ductile shear zones predate a cracking front, whereas at fast-spreading rates, ductile shear zones are absent, and permeability should initially be generated solely by the cracking front. Mével and Cannat (1991) assumed a constant temperature of 500 °C for the inception of fracturing, regardless of depth in the crust.

Our observations of the earliest fracturing in Hess Deep and Wadi Abyad gabbros produced by fast spreading support the idea that water penetration and initial brittle failure are related and that this process can affect the entire crustal section. In both gabbro localities, the earliest metamorphic fluid + rock reactions are texturally related to fractures. However, the Oman and East Pacific Rise gabbros require revision of the Lister model and its subsequent modifications in several fundamental ways, including cracking scale, temperature, and nature of the front propagation. These differences provide constraints on the nature of heat transport and fracture evolution in the lower oceanic crust in fast-spreading environments.

Scale of fracturing. A key feature of the Lister model is that initial fracturing is postulated to occur as widely spaced cracks with significant lateral extents and spacings of centimeters to meters; that is, within the brittle regime of cataclastic faulting and strain localization (e.g., Rutter, 1986; Evans et al., 1990). In the model, water first penetrates "a semi-infinite expanse of hot rock at a planar 'cracking front,' it being understood that the cracks are *macrocracks* on a scale of several centimeters and nothing like the 'microfracturing' associated with brittle creep" (Lister, 1974, p. 470). Lister (1974) was interested in the possibility of fracture-controlled advective heat transport, so he focused his attention on the brittle-faulting regime where permeability is likely to be higher for longer times. Although he may not have intended his analysis to be applied strictly to the entire subsolidus deformation history, it has nevertheless gained wide currency in the literature as a guide to the links between deformation and metamorphism of the oceanic crust. Thus it is important to emphasize that our observations demonstrate that initial fracture deformation of lower-crustal oceanic rocks is actually semibrittle in character. There is minimal strain localization. Instead, the structures are distributed, dilatant microcracks found predominantly in grain-boundary regions.

Lister (1974) also proposed that the fracture system should coalesce with time via "pattern enlargement." Although different in scale, the fracture systems do show evidence for increasing degree of strain localization, which we take to be synonymous with Lister's "pattern enlargement." In Hess Deep, microfractures are crosscut by the earliest set of macroscopic fractures, which are filled by the same minerals (Manning and MacLeod, 1996). The macroscopic fractures are less abundant and more continuous than their microscopic counterparts. This finding is consistent with the channeling of fluids into fewer and larger conduits. Weston (1998) showed that the macroscopic amphibole fractures formed at only slightly lower temperatures (704–674 °C), a distinction that is statistically significant at the 90% confidence level. This result implies that the fracture system associated with the cracking front can locally evolve from pervasively distributed microcracks to larger, throughgoing fractures over a narrow temperature interval, though these larger fractures are comparatively rare (Manning and MacLeod, 1996). This textural evolution is consistent with a progressive change from semibrittle, cataclastic flow to brittle, cataclastic faulting with time and declining temperature.

Cracking temperature. The second difference between the observed initial fracture system and the Lister model is the temperature of cracking and its distribution with depth. Lister (1974) assumed that failure by transient creep would occur at a strain rate of $\sim 3 \times 10^{-8}$ s^{-1} after build up of 1%–2% plastic strain during cooling. As lithostatic pressure increases, greater strains—and, hence, lower temperatures—occur before cracking. Figure 4 illustrates Lister's (1974) estimate of the cracking temperature by using his parameter choices, a water-column depth of 2.5 km, 2 km of basalts and dikes overlying gabbros, and rock density of 3000 kg/m^3. The curve in Figure 4 corresponds to the depth at which stress at failure is equal to confining pressure (the Goetze criterion for the brittle-plastic transition). It therefore represents the maximum model cracking temperature at any depth. At the dike-gabbro transition, the maximum cracking temperature in this scenario would be 650 °C; at the Oman Moho, 550 °C.

Our calculated temperatures for initial microfracturing at any position within the gabbros are higher than those predicted by Lister (1974) by ~65 to ~275 °C (Fig. 4), or ~10%–50%. What is more important, calculated temperatures increase instead of decrease with depth. This discrepancy is independent of assumed flow law or strain rate. For example, Hirth et al. (1998) used various flow laws at the

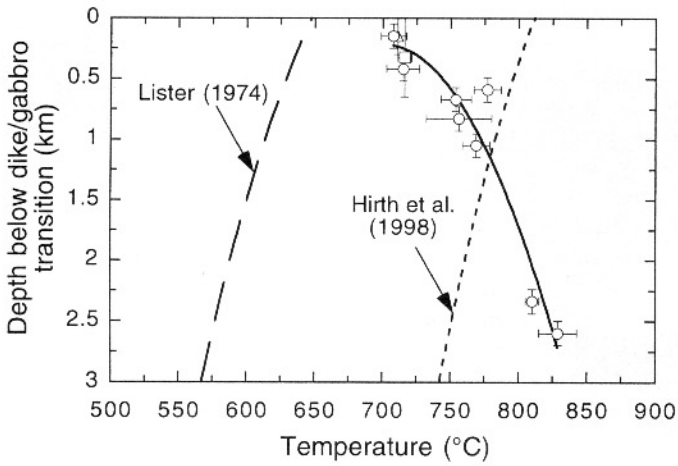

Figure 4. Comparison of observed temperature distribution with predicted position of the cracking front of Lister (1974) and the brittle-plastic transition of Hirth et al. (1998) based on the Mackwell et al. (1998) flow law for dry Maryland diabase at a strain rate of 10^{-14} s^{-1}.

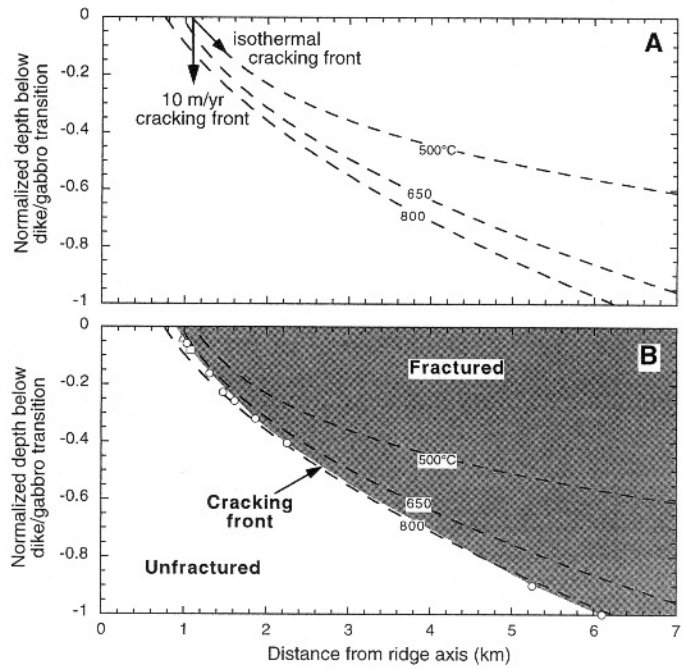

Figure 5. Variation in temperature of cracking front with depth and distance from ridge axis. Isotherms are taken from Phipps Morgan and Chen (1993) model results for a spreading rate of 50 mm/yr. Thicknesses of Oman gabbros (2.6 km), Hess Deep gabbros (assumed to be 4 km), and the model (4 km) were normalized to unity for comparison. A, Arrows show that propagation velocity of 10 m/yr at a specific locality will result in metamorphic temperatures spanning many hundreds of degrees, whereas isothermal cracking requires that the front moves downward and away from the ridge axis at a shallow angle. B, Results of this study compared to the thermal model show that the cracking front in crust formed in a fast-spreading environment occurs at progressively higher temperatures with increasing depth in the crust, requiring that fracturing occurs over a distance of several kilometers between 1 and 6 km from the ridge axis. The region that has been affected by a high-temperature cracking front is shaded. Symbols as in Figure 3.

lower strain rate of 10^{-14} s^{-1} to predict the temperature of the brittle-plastic transition in the oceanic lower crust. All are similar in form to the Lister curve. Figure 4 shows the brittle-plastic transition for the dry-Maryland-diabase flow law of Mackwell et al. (1998). Our calculated cracking temperatures lie within the brittle field from 0 to 1 km below the dike-gabbro transition; however, near the Oman Moho, calculated cracking temperatures are above the brittle-plastic transition of Hirth et al. (1998). Figure 4 illustrates that the increase in cracking temperature with depth is not consistent with failure along a front defined by the boundary between brittle and plastic deformation mechanisms for the Mackwell et al. (1998) flow law and a constant strain rate.

There are two possible explanations for the observed increase in the temperature of semibrittle deformation with depth. First, fracturing may not correspond to the brittle-plastic transition at all depths. In this scenario, the maximum stress difference encountered by the rocks was below their failure strength at the brittle-plastic transition and remained so until the yield strength was exceeded at lower temperatures. However, this scenario should produce a more random distribution of cracking temperature with depth, not the observed systematic change that is evidently independent of gabbro locality. Alternatively, the metamorphic temperatures correspond very nearly to the brittle-plastic transition, but their variation with depth indicates rheologic differences corresponding to changes in modal abundance of magmatic minerals such as olivine, increasing extent of hydrolytic weakening with depth, or increasing strain rate with depth. Because a strain-rate increase with depth is a necessary consequence of viscous flow of crust away from the ridge axis (e.g., Chen and Morgan, 1990; Quick and Denlinger, 1993; Chenevez et al., 1998), it is a strong candidate for explaining the observed variation between temperature and depth, though the other alternatives cannot be ruled out.

Propagation of the cracking front. Lister (1974, 1982) suggested that the cracking front can advance downward at the rate of tens of meters per year at all depths. Even at fast spreading rates, such rapid propagation velocities would allow penetration through the entire crustal section over very short distances normal to the spreading direction. For example, at 65 mm/yr (the spreading rate of the East Pacific Rise at the latitude of Hess Deep; Francheteau et al., 1990), a front velocity of 10 m/yr would result in penetration to the base of a hypothetical 6 km crustal section in 600 yr while the crust spread laterally 39 m. Figure 5A shows that these propagation velocities would effectively mean instantaneous penetration of the entire crust. If fracturing of the lower crust were to occur in a single such event, temperatures of cracking and metamorphism would increase with depth in the crust by many hundreds of degrees across an entire crustal section. Because Lister (1974) inferred a narrow temperature interval for fracturing, he proposed that the rapid front velocities required episodic cracking events progressively farther from the ridge axis. For an isothermal front (Mével and Cannat, 1991), the distance from ridge axis at which fracturing occurred could exceed 10 km if temperatures were ≤500 °C (Fig. 5A).

Initial fracturing in Oman and Hess Deep gabbros displays a slight increase in temperature with depth, requiring a small but significant (~100 °C) transgression of isotherms and cracking progressively more distant from the ridge axis. The rate of spreading at which Oman crust was produced, although likely rapid, is unknown in detail. However, if a rate similar to that inferred for Hess Deep is assumed, then a schematic sense of the implications of our observations can be gained through integration with thermal models, such as those of Phipps Morgan and Chen (1993). Figure 5B illustrates that the fracturing near the dike-gabbro transition would occur at ~1

km from the spreading axis, but at ~6 km at Moho depths. If cracking proceeded downward along a continuously propagating front, the penetration velocity would have been 34 mm/yr. This is slower than the spreading rate by a factor of nearly two and slower than the velocity inferred by Lister (1974) by about three orders of magnitude. When combined with the rapid reaction rates at the high temperatures inferred for cracking, the low apparent propagation velocity and the wide range in distance from the ridge axis suggest that initial semibrittle microcracking is episodic.

The inference that initial microfracturing is episodic has important implications for the subsolidus evolution of deformation and metamorphism in the lower crust. If the first microfractures at any depth are connected to shallower fracture systems, then the cumulative effect of the successive cracking required to deepen the front would be to produce a virtually continuous record of metamorphism from the upper-amphibolite facies to lower metamorphic grades. Such a record may be shown to some extent by the later chlorite observed in the north-scarp gabbros of Hess Deep (e.g., Gillis, 1995). But late chlorite is not a general feature of the deeper gabbro metamorphism in either locality. Instead, the early microfractures form at high temperatures, and locally coalesce into larger fracture systems now represented by hornblende veins. The crack arrays are open for short times over narrow temperature intervals (Manning and MacLeod, 1996; Manning et al., 1996; Weston, 1998). The rocks then cool over significant temperature intervals during which little metamorphism occurs, until fractures filled by greenschist-facies minerals are generated. Thus, the continuous record of metamorphism that should exist if multiple cracking events of substantial vertical extent were to cut the gabbros has not been observed. This finding leads to two possibilities for fracture evolution in the lower crust of fast-spreading environments: (1) cooling through the interval of initial cracking into the greenschist facies (~500 °C) is so rapid (Fig. 5) that the structures formed at these conditions are rare and have gone unrecognized, or (2) there is limited vertical connectivity to the initial microfracture systems. Distinguishing between these two possibilities is not possible on the basis of currently available data.

Heat transport and later, macroscopic fracture systems. The nature of heat transport during semibrittle microfracturing can be determined by considering the temperature of metamorphism and the compositions of secondary minerals. Statistical analysis of temperatures in Hess Deep samples implies that metamorphism occurred over a narrow temperature interval, below which no further amphibolite-facies metamorphism took place (Manning et al., 1996). The standard deviations of the temperatures for each Oman sample suggest that this statement is true for that suite as well. Given the rapid cooling rates expected for gabbros formed in fast-spreading environments (Fig. 5), metamorphism over a limited temperature range implies that fluid flow associated with the cracking front was short-lived. Moreover, the limited degree of homogenization of amphibole compositions in Hess Deep (Manning and MacLeod, 1996) and Oman (this study) suggests that cracks sealed rapidly compared to the rate of transport of chemical components. These lines of evidence imply that fluid flux is low and that the lower crust therefore cools conductively through the amphibolite facies (down to 500 °C). This result contrasts with the Lister (1974) model of the cracking front, where the onset of fracturing brings the crust into a new regime of hydrothermal cooling, in which heat is transported advectively by fluids flowing in long-lived cracks.

Although the earliest fracturing in Oman and East Pacific Rise gabbros differs in many respects from the idealized crack system postulated by Lister, later vein sets may be more similar. In both localities, later veins are longer (meters to tens of meters), are lower temperature (predominantly greenschist facies), and have spacings of centimeters to meters. If these fractures were open for long times, they may have allowed advection of thermal energy out of the lower crust. However, our observations suggest that such fracture systems developed in already cracked and hydrated crust.

CONCLUSIONS

The earliest fracturing in gabbros from fast-spreading environments such as at Hess Deep and Wadi Abyad, Oman, is defined by a semibrittle, distributed microcrack-network that is filled by hornblende. Our observations show that initial tensile failure is the event that first allows water penetration into the lower oceanic crust. This process can affect the entire crustal section. The temperatures of initial fracturing are high and increase with depth, from ~700 °C at the dike-gabbro transition to ~825 °C at the Oman Moho. Microfracturing occurred at increasing distance from the ridge axis with progressively greater depths in the gabbros. The actual distance depends on thermal structure and spreading rate. If the models of Phipps Morgan and Chen (1993) are representative, then initial fracturing occurred at ~1 km from the ridge axis at the dike-gabbro transition and at ~6 km at the Oman Moho. Microfracturing is probably episodic because the velocity required for continuous downward propagation is slow relative to expected reaction rates. The temperature data suggest that cracking occurred at increasing strain rate with depth, that the rheologic properties of the layered, foliated, and variably textured gabbros varied with depth, or that the effects of water on strength led to progressive weakening with depth. The microscopic scale and heterogeneity of amphibole compositions imply limited fluid flow, which suggests that heat flow was conductive during early metamorphism.

ACKNOWLEDGMENTS

Supported by National Science Foundation grants OCE-9405999 and 9529602 (to Manning). Reviews by K. Gillis, R. Ingersoll, D. Stakes, and R. Newton improved the manuscript.

REFERENCES CITED

Benn, K., and Allard, B., 1989, Preferred mineral orientations related to magmatic flow in ophiolite layered gabbros: Journal of Petrology, v. 30, p. 925–946.

Beurrier, M., 1988, Geologie de la nappe ophiolitique de Semail dans les parties orientale et centrale de l'Oman: Paris, Université de Paris Bureau de Recherches Geologiques et Minieres, v. 128, 412 p.

Boudier, F., Nicolas, A., and Ildefonse, B., 1996, Magma chambers in the Oman ophiolite: Fed from the top and the bottom: Earth and Planetary Science Letters, v. 144, p. 239–250.

Brabander, D.J., and Giletti, B.J., 1995, Strontium diffusion kinetics in amphiboles and significance to thermal history determination: Geochimica et Cosmochimica Acta, v. 59, p. 2223–2238.

Browning, P., 1982, The petrology, geochemistry, and structure of the plutonic rocks of the Oman Ophiolite [Ph.D. thesis]: Milton Keynes, The Open University, 404 p.

Browning, P., 1984, Cryptic variation within the cumulate sequence of the Oman ophiolite: Magma chamber depth and petrological implications, *in* Gass, I.G., Lippard, S.J., and Shelton, A.W., eds., Ophiolites and oceanic lithosphere: Geological Society of London Special Publication 14, p. 71–82.

Chen, Y., and Morgan, W.J., 1990, A nonlinear rheology model for mid-ocean ridge axis topography: Journal of Geophysical Research, v. 95, p. 17583–17604.

Chenevez, J., Machetel, P., and Nicolas, A., 1998, Numerical models of magma chambers in the Oman ophiolite: Journal of Geophysical Research, v. 103, p. 15443–15455.

Ernewein, M., Pflumio, C., and Whitechurch, H., 1988, The death of accretion zone as evidenced by the magmatic history of the Sumail ophiolite (Oman): Tectonophysics, v. 151, p. 247–274.

Evans, B., Frederich, J.T., and Wong, T.-F., 1990, The brittle-ductile transition in rocks: Recent experimental and theoretical progress, *in* Duba, A.G., Durham, W.B., Handin, J.W., and Wang, H.F., eds., The brittle-ductile transition in rocks: New York, American Geophysical Union Monograph, v. 56, p. 1–20.

Francheteau, J., Armijo, R., Cheminée, J.L., Hekinian, R., Lonsdale, P., and Blum, N., 1990, 1 Ma East Pacific Rise oceanic crust and uppermost mantle exposed by rifting in Hess Deep (equatorial Pacific Ocean): Earth and Planetary Science Letters, v. 101, p. 281–295.

Giletti, B.J., and Casserly, J.E.D., 1994, Strontium diffusion kinetics in plagioclase feldspars: Geochimica et Cosmochimica Acta, v. 58, p. 3785–3793.

Giletti, B.J., and Shananan, T.M., 1997, Alkali diffusion in plagioclase feldspar: Chemical Geology, v. 139, p. 3–20.

Gillis, K.M., 1995, Controls on hydrothermal alteration in a section of fast-spreading oceanic crust: Earth and Planetary Science Letters, v. 134, p. 473–489.

Gillis, K.M., Mével, C., Allan, J., and the Leg 147 Scientific Party, 1993, Proceedings of the Ocean Drilling Program, Initial Reports, v. 147: College Station, Texas, Ocean Drilling Program, 366 p.

Gillis, K.M., Thompson, G., and Kelley, D.S., 1993, A view of the lower crustal component of hydrothermal systems at the Mid-Atlantic Ridge: Journal of Geophysical Research, v. 98, p. 19597–19619.

Gregory, R.T., and Taylor, H.P., Jr., 1981, An oxygen isotope profile in a section of Cretaceous oceanic crust, Samail ophiolite, Oman: Evidence for $\delta^{18}O$ buffering of the oceans by deep (>5 km) seawater-hydrothermal circulation at mid-ocean ridges: Journal of Geophysical Research, v. 86, p. 2737–2755.

Helz, R.H., 1973, Phase relations of basalts in their melting range at P_{H_2O} = 5 kb as a function of oxygen fugacity: Journal of Petrology, v. 14, p. 249–302.

Hirth, G., Escartin, J., and Lin, J., 1998, The rheology of the lower oceanic crust: Implications for lithospheric deformation at mid-ocean ridges, *in* Buck, W.R., Delaney, P.T., Karson, J.A., and Lagabrielle, Y., eds., Faulting and magmatism at mid-ocean ridges: New York, American Geophysical Union Monograph, v. 106, p. 291–303.

Holland T.J.B., and Blundy, J.D., 1994, Non-ideal interactions in calcic amphiboles and their bearing on amphibole-plagioclase thermometry: Contributions to Mineralogy and Petrology, v. 116, p. 433–447.

Jenkins, D.M., 1987, Synthesis and characterization of tremolite in the system H_2O-CaO-MgO-SiO_2: American Mineralogist, v. 72, p. 707–715.

Juteau, T., Beurrier, M., Dahl, R., and Nehlig, P., 1988, Segmentation at a fossil spreading axis: The plutonic sequence of the Wadi Haymiliayah area (Haylayn Block, Sumail Nappe, Oman): Tectonophysics, v. 151, p. 167–197.

Karson, J.A., Hurst, S.D., and Lonsdale, P.F., 1992, Tectonic rotations of dikes in fast-spread oceanic crust exposed near Hess Deep: Geology, v. 20, p. 685–688.

Leake, B.E., 1978, Nomenclature of amphiboles: Canadian Mineralogist, v. 16, p. 501–520.

Lécuyer, C., and Gruau, G., 1996, Oxygen and strontium isotope compositions of Hess Deep gabbros (Holes 894F and G): High-temperature interaction of seawater with the oceanic crust layer 3: Proceedings of the Ocean Drilling Program, Scientific Results, v. 147: College Station, Texas, Ocean Drilling Program, p. 227–234.

Lippard, S.J., Shelton, A.W., and Gass, I.G., 1986, The ophiolite of northern Oman: Geological Society of London Memoir 11, 178 p.

Lister, C.R.B., 1974, On the penetration of water into hot rock: Geophysical Journal of the Royal Astronomical Society, v. 39, p. 465–509.

Lister, C.R.B., 1982, "Active" and "passive" hydrothermal systems in the oceanic crust: Predicted physical conditions, *in* Fanning, K.A., and Mannheim, F.T., eds., The dynamic environment of the ocean floor: Lexington, Massachusetts, D.C. Heath, p. 441–459.

Liu, M., and Yund, R.A., 1992, NaSi-CaAl interdiffusion in plagioclase: American Mineralogist, v. 77, p. 275–283.

Lonsdale, P., 1988, Structural pattern of the Galapagos Microplate and evolution of the Galapagos triple junctions: Journal of Geophysical Research, v. 93, p. 13551–13574.

Mackwell, S.J., Zimmerman, M.E., and Kohlstedt, D.L., 1998, High-temperature deformation of dry diabase with application to tectonics of Venus: Journal of Geophysical Research, v. 103, p. 975–984.

MacLeod, C.J., and Rothery, D.A., 1992, Ridge axial segmentation in the Oman ophiolite: Evidence from along-strike variations in the sheeted dyke complex, *in* Parson, L.M., Murton, B.J., and Browning, P., eds., Ophiolites and their modern oceanic analogues: Geological Society of London Special Publication 60, p. 39–63.

MacLeod, C.J., and Yaouancq, G., 2000, A fossil melt lens in the Oman ophiolite: Implications for magma chamber processes at fast-spreading ridges: Earth and Planetary Science Letters, v. 176, p. 357–373.

MacLeod, C.J., Boudier, F., Yaouancq, G., and Richter, C., 1996, Gabbro fabrics from ODP Site 894, Hess Deep: Implications for magma chamber processes at the East Pacific Rise: Proceedings of the Ocean Drilling Program, Scientific Results, v. 147: College Station, Texas, Ocean Drilling Program, p. 317–328.

Manning, C.E., and MacLeod, C.J., 1996, Fracture-controlled metamorphism of Hess Deep Gabbros, Site 894: Constraints on the roots of mid-ocean ridge hydrothermal systems at fast spreading centers: Proceedings of the Ocean Drilling Program, Scientific Results, v. 147: College Station, Texas, Ocean Drilling Program, p. 189–212.

Manning, C.E., Weston, P.E., and Mahon, K.I., 1996, Rapid high-temperature metamorphism of East Pacific Rise gabbros from Hess Deep: Earth and Planetary Science Letters, v. 144, p. 123–132.

Mével, C., and Cannat, M., 1991, Lithospheric stretching and hydrothermal processes in oceanic gabbros from slow-spreading ridges, *in* Peters, T., Nicolas, A., and Coleman, R.G., eds., Ophiolite genesis and evolution of the oceanic lithosphere: Dordrecht, Netherlands, Kluwer Academic Publishers, p. 293–312.

Natland, J.H., and Dick, H.J.B., 1996, Melt migration through high-level gabbroic cumulates of the East Pacific Rise at Hess Deep: Inferences from rock textures and mineral compositions: Proceedings of the Ocean Drilling Program, Scientific Results, v. 147: College Station, Texas, Ocean Drilling Program, p. 21–58.

Nehlig, P., 1994, Fracture and permeability analysis in magma-hydrothermal transition zones in the Samail ophiolite (Oman): Journal of Geophysical Research, v. 99, p. 589–601.

Nehlig, P., and Juteau, T., 1988a, Flow porosities, permeabilities, and preliminary data on fluid inclusions and fossil thermal gradients in the crustal sequence of the Sumail ophiolite (Oman): Tectonophysics, v. 151, p. 199–221.

Nehlig, P., and Juteau, T., 1988b, Deep crustal seawater penetration and circulation at ocean ridges: Evidence from the Oman ophiolite: Marine Geology, v. 84, p. 209–228.

Nicolas, A., 1989, Structures of ophiolites and dynamics of oceanic lithosphere: Boston, Kluwer Academic Publishers, 367 p.

Nicolas, A., 1992, Kinematics in magmatic rocks with special reference to gabbros: Journal of Petrology, v. 33, p. 891–915.

Nicolas, A., and Boudier, F., 1995, Mapping oceanic ridge segments in Oman ophiolite: Journal of Geophysical Research, v. 92, p. 6179–6197.

Nicolas, A., Reuber, I., and Benn, K., 1988, A new magma chamber model based on structural studies in the Oman ophiolite: Tectonophysics, v. 151, p. 87–105.

Nicolas, A., Boudier, F., and Ildefonse, B., 1994, Evidence from the Oman ophiolite for active mantle upwelling beneath a fast-spreading ridge: Nature, v. 370, p. 51–53.

Pallister, J.S., and Hopson, C.A., 1981, Samail plutonic suite: Field relations, phase variations, cryptic variation and layering, and a model of a spreading ridge magma chamber: Journal of Geophysical Research, v. 86, p. 2593–2644.

Phipps Morgan, J., and Chen, Y.J., 1993, The genesis of oceanic crust: Magma injection, hydrothermal circulation, and crustal flow: Journal of Geophysical Research, v. 98, p. 6283–6297.

Pouchou, J.L., and Pichoir, J.F., 1986, Very high elements X-ray-microanalysis—recent models of quantification: Journal de Microscopie et de Spectroscopie Electroniques, v. 11, p. 229–250.

Quick, J.E., and Denlinger, R.P., 1993, Ductile deformation and the origin of layered gabbro in ophiolites: Journal of Geophysical Research, v. 98, p. 14015–14027.

Reuber, I., Nehlig, P., and Juteau, T., 1991, Axial segmentation at a fossil oceanic spreading centre in the Haylayn block (Semail nappe, Oman): Off-axis

mantle diapir and advancing ridge tip: Journal of Geodynamics, v. 13, p. 253–278.

Rothery, D.A., 1983, The base of a sheeted dyke complex, Oman ophiolite: Implications for magma chambers at oceanic spreading axes: Journal of the Geological Society of London, v. 140, p. 287–296.

Rutter, E.H., 1986, On the nomenclature of mode of failure transitions in rocks: Tectonophysics, v. 122, p. 381–387.

Simmons, G., and Richter, D., 1976, Microcracks in rocks, *in* Strens, R.G.J., ed., The physics and chemistry of minerals and rocks: London, Wiley, p. 105–137.

Spear, F.S., 1981, An experimental study of hornblende stability and compositional variability in amphibolite: American Journal of Science, v. 281, p. 697–734.

Stakes, D.S., and Taylor, H.P., Jr., 1992, The northern Samail ophiolite: An oxygen isotope, microprobe, and field study: Journal of Geophysical Research, v. 97, p. 7043–7080.

Stakes D.S., and Vanko, D.A., 1986, Multistage hydrothermal alteration of gabbroic rocks from the failed Mathematician Ridge: Earth and Planetary Science Letters, v. 79, p. 75–92.

Stakes, D.S., Mével, C., Cannat, M., and Chaput, T., 1991, Metamorphic stratigraphy of Hole 735B: Proceedings of the Ocean Drilling Program, Scientific Results, v. 118: College Station, Texas, Ocean Drilling Program, p. 153–180.

Tilton, G.R., Hopson, C.A., and Wright, J.E., 1981, Uranium-lead isotopic ages of the Samail ophiolite, Oman, with application to Tethyan ocean ridge tectonics: Journal of Geophysical Research, v. 86, p. 2763–2776.

Walther, J.V., and Wood, B.J., 1984, Rate and mechanism in prograde metamorphism: Contributions to Mineralogy and Petrology, v. 88, p. 246–259.

Weston, P.E., 1998, Temperature, timing, and fluid composition constraints for high temperature fracturing and hydrous mineral formation in gabbros from Hess Deep [M.S. thesis]: Los Angeles, University of California at Los Angeles, 152 p.

Wilks, K.R., and Carter, N.L., 1986, Ductile and semi-brittle deformations of layer 3 gabbros: Zambales, Bay of Islands, and Samail ophiolites: Eos, Transactions of the American Geophysical Union, v. 67, p. 1202.

Wood, B.J., and Walther, J.V., 1983, Rates of hydrothermal reactions: Science, v. 222, p. 413–415.

Manuscript Accepted by the Society February 23, 2000